

**Robert G. Parker<sup>1</sup>**

Associate Professor  
e-mail: parker.242@osu.edu

**Vinayak Agashe**

Department of Mechanical Engineering,  
The Ohio State University,  
206 W. 18th Ave.,  
Columbus, OH 43201-1107

**Sandeep M. Vijayakar**

Advanced Numerical Solutions,  
3554 Mark Twain Ct.,  
Hilliard, OH 43026

# Dynamic Response of a Planetary Gear System using a Finite Element/Contact Mechanics Model

*The dynamic response of a helicopter planetary gear system is examined over a wide range of operating speeds and torques. The analysis tool is a unique, semianalytical finite element formulation that admits precise representation of the tooth geometry and contact forces that are crucial in gear dynamics. Importantly, no a priori specification of static transmission error excitation or mesh frequency variation is required; the dynamic contact forces are evaluated internally at each time step. The calculated response shows classical resonances when a harmonic of mesh frequency coincides with a natural frequency. However, peculiar behavior occurs where resonances expected to be excited at a given speed are absent. This absence of particular modes is explained by analytical relationships that depend on the planetary configuration and mesh frequency harmonic. The torque sensitivity of the dynamic response is examined and compared to static analyses. Rotational mode response is shown to be more sensitive to input torque than translational mode response. [S1050-0472(00)00403-7]*

## 1 Introduction

Planetary gears yield several advantages over conventional parallel shaft gear systems. They produce high speed reductions in compact spaces, greater load sharing, higher torque to weight ratio, diminished bearing loads and reduced noise and vibration. They are used in automobiles, helicopters, aircraft engines, heavy machinery, and a variety of other applications. Despite their advantages, the noise induced by the vibration of planetary gear systems remains a key concern. In helicopters, for example, cabin noise exceeding 100 dB is directly traceable to the last stage planetary gear mounted to the cabin.

Planetary gears have received considerably less research attention than single mesh gear pairs. There is a particular scarcity of *dynamic response* calculations. The purpose of this work is to characterize the dynamic response of a planetary gear system under a wide range of operating conditions. The analytical technique combines a unique, semi-analytical finite element approach with detailed contact modeling at the tooth mesh. This approach was specifically developed to examine the mechanics of precisely-machined, contacting elastic bodies such as gears. The semi-analytical finite element formulation does not require a highly refined mesh at the contacting tooth surfaces. This dramatically reduces the computational effort and allows calculation of the *dynamic response* at a sufficient number of time steps to study the response in the frequency domain. In contrast, the need for extremely refined gear tooth meshes limits conventional finite element analysis to static analyses and free vibration eigensolutions. The current analysis provides a more accurate and comprehensive study of planetary gear dynamic response than is reasonably possible, or has been conducted, with conventional finite element analysis.

Experimental measurement of planetary gear dynamic response under operating conditions is difficult due to the limited access and multiple moving bodies. As a result, few benchmark experimental results suitable for dynamic model validation have been

published. In fact, comprehensive planetary gear dynamic response analyses are notably lacking in the literature. While the present work is still subject to a number of modeling idealizations, the modeling has higher fidelity representation of the dynamic excitations and tooth contact mechanics than published models. In this regard, the presented results provide a benchmark for further development of planetary gear dynamic models.

The literature on planetary gear mechanics emphasizes highly idealized lumped parameter modeling wherein the gears are rigid bodies interconnected by springs representing meshing teeth and support bearings. For free vibration analyses, see [1–6]. Kahraman [7,8] used two- and three-dimensional models to examine the dynamic response of both time-invariant and time-varying representations. Vexex and Flamand [9] used lumped modeling [10] and a Ritz approach to examine the dynamic response induced by mesh parametric excitations. In all these studies, the gear bodies are represented using lumped parameter models. Valco [11] used a non-linear finite element model of a planetary gear system to calculate stresses, strains and deformations in the gear bodies under static loading; dynamic response is not considered. Gradu et al. [12] used a finite element model to obtain the dynamic response of various planetary gear systems with different planet spacings. The dynamic excitation, which is typically not well-known, must be specified externally in that model.

## 2 Finite Element/Contact Mechanics Model

The sun gear speed is specified and the nominal rigid body motions of the components are determined according to basic planetary gear kinematics; the calculated outputs are the component vibrational motions superposed on this large motion. The analysis is *not* of a single, fixed configuration; the teeth continuously enter and exit contact at each mesh as the gears rotate, and the resulting dynamic forces are computed by a thorough contact analysis. *It is not necessary to externally specify the time-varying mesh stiffness and mesh contact forces as they are evaluated internally at each time step.* These internally calculated quantities comprise the complete dynamic excitation. This contrasts sharply with typical gear models that require a priori specification of the mesh stiffness variation and static transmission error as the dy-

<sup>1</sup>Corresponding author.

Contributed by the Power Transmission & Gearing Committee for publication in the JOURNAL OF MECHANICAL DESIGN. Manuscript received May 1999. Associate Technical Editor: R. F. Handschuh.

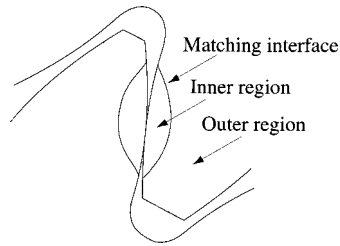


Fig. 1 Contact region division into inner and outer regions

dynamic excitations. Such methods are difficult to apply in planetary gears because these fundamental dynamics excitations are difficult to measure or estimate.

The geometric surface description of the meshing teeth must be very precise for gear applications. Additionally, the contact region is narrow and travels over the entire tooth surface. Conventional finite element analyses require a prohibitively refined mesh to address these problems when one seeks dynamic response. The current model addresses these issues by using a combination of the Bousinesq solution for a point load acting on a half-space and traditional finite element analysis to exploit the advantages of each [13].

The approach relies on a division of the tooth into inner and outer regions where each solution applies (Fig. 1). In brief, the Bousinesq solution and contact forces are integrated over the tooth contact region like a Green's function to accurately represent relative displacements in an inner region close to the tooth surface, though absolute displacements will not be accurate because of overall tooth bending about the root. Outside the immediate vicinity of the contact zone, finite element analysis effectively models the elastic body response, including gross deflections associated with tooth bending. The Bousinesq and finite element solutions are matched along an interface close to the tooth surface to yield a solution accurate in both the inner and outer regions. The matching surface is chosen 1) sufficiently far from the tooth boundaries so that the finite domain does not affect the inner region relative displacements, and 2) sufficiently far from the contact surface that the outer region finite elements can accurately capture the reduced strain gradients away from the contact zone. The inner half-space and outer finite element solutions are matched as follows to yield the total displacement in the inner region

$$u_{\text{inner}}(r) = [u_{hs}(r) - u_{hs}(q)] + u_{fe}(q) \quad (1)$$

The bracketed term on the right-hand side is the relative displacement of an inner point  $r$  with respect to a point  $q$  on the matching surface; it is evaluated using the integrated half-space solution. The second term is evaluated using conventional finite element analysis. The displacements of points in the outer region are obtained purely from finite element analysis. The result is a continuum approximation in the localized contact region and a finite element discretization over the remainder of the body. The remarkable advantage for gear dynamics is that the meshes do not require unusual refinement near the tooth surface to capture the contact mechanics and steep strain gradients.

Furthermore, the tooth surface geometry is not specified by conventional element edges. Rather, special finite elements [13] which allow  $C^1$  continuous representation of the tooth surface are used for elements on the contacting tooth surfaces. The shape functions for these special elements are defined using Hermite polynomials whose coefficients are chosen such that the tooth surfaces are represented to arbitrary precision within prescribed tooth surface tolerances. This is essential as precise tooth surface definition is critical when one seeks dynamic response. Because the tooth surface geometry is not defined by the conventional finite element nodes, accurate representation of the tooth surface

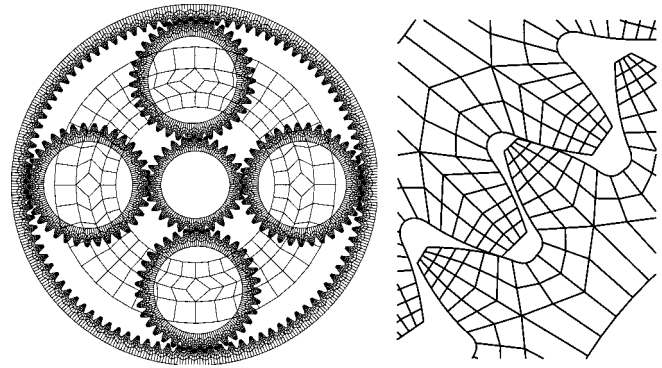


Fig. 2 Finite element mesh for the planetary gear system

is possible with a relatively coarse mesh, i.e., a side of the tooth surface is modeled precisely using just seven elements (Fig. 2). Four-noded, linear finite elements are used for the carrier and sections of the gear bodies not on the tooth surface.

A contact analysis at each time step determines the contact stresses and the deformation of the gear bodies. The deformations and load distributions under dynamic conditions are obtained by solving the matrix equation of motion  $M\ddot{x} + C\dot{x} + Kx = f$ .  $M$ ,  $C$  and  $K$  represent mass, damping and stiffness matrices for the system. A constant external sun gear torque acting on the system is included in the form of an external forcing vector  $f$ . Structural damping is idealized as proportional viscous damping. The unconditionally stable Newmark method is used for time integration of the equations of motion with 141 time steps per tooth mesh cycle. Contact constraints are imposed on the discretized matrix equations, and the system is solved by the simplex algorithm [14]. The simplex algorithm is widely used to solve linear and quadratic programming problems.

To experimentally validate the formulation described above, a separate study was conducted [15] to examine the dynamic response of a spur gear pair. The results were remarkably consistent with experimental measurements [16], including excellent predictions of nonlinear jump phenomena and superharmonic resonances.

The mesh for the Army OH-58 Kiowa helicopter planetary gear used throughout this study is shown in Fig. 2. The parameters are given in Table 1, and pictures are provided in [17]. The inner circles of the sun, planet, and carrier meshes and the diamond shapes of the carrier represent rigid bearing races restrained by isotropic, linear bearing springs of stiffness  $87.6 \times 10^6$  N/m ( $0.5 \times 10^6$  lb/in). Translation and rotation of these races represent the overall gear vibrations and are the quantities presented subsequently. The outer ring gear circle is rigidly fixed. Only planar motions are considered in this two-dimensional model where all gears have a facewidth of 25.4 mm (1 in). Light bearing viscous

Table 1 Gear data for the Army OH-58 Kiowa planetary gear-set

Gear Data	Sun	Ring	Planet
Number of Teeth	27	99	35
Base Circle Diam. (mm)	70.40	258.1	91.26
Inner/Major Diam. (mm)	57.15/84.07		73.66/105.0
Outer/Minor Diam. (mm)		304.8/271.8	
Root Diam. (mm)	70.55	284.1	91.54
Pressure Angle (deg)	24.60	20.19	
Module (mm)	2.868	2.778	

damping is specified to minimize the computational effort required to attain steady state dynamic response. All gears are steel spur gears with Young's modulus =  $207 \times 10^9$  N/m<sup>2</sup>, density =  $7595$  kg/m<sup>3</sup>, and Poisson's ratio =  $0.3$ . The teeth are unmodified from perfect involutes. Two different systems having either three or four planet gears are examined; the sun, ring and planet gears are identical in both configurations. While the planets are equally spaced for the three planet case, those in the four planet case are unequally spaced at  $\psi_i = 0, -88.6, 180,$  and  $91.4$  deg. The input torque is specified at the sun gear, and the output power is through the carrier. The carrier rotational vibration is constrained to zero, i.e., the carrier rotation is exactly according to its nominal kinematic position and the output torque fluctuates about the nominal value of output torque.

### 3 Natural Frequencies and Vibration Modes

Lin and Parker [4,5] rigorously analyzed the structure of the natural frequency spectrum and vibration modes of general planetary gear systems using a lumped parameter model. They characterized the vibration modes into three classes:

- 1 *Translational modes* in which the sun, carrier and ring have only translational motion and no rotational motion;
- 2 *Rotational modes* in which the sun, carrier and ring have only rotational motion and no translational motion; and
- 3 *Planet modes* in which the sun, carrier, and ring have no motion and only the planets deflect.

In this analysis, computational modal tests that simulate experimental impact testing are performed on the stationary system. The impulses are forces and torques applied for a single time step. The frequency content of the transient dynamic response is studied to

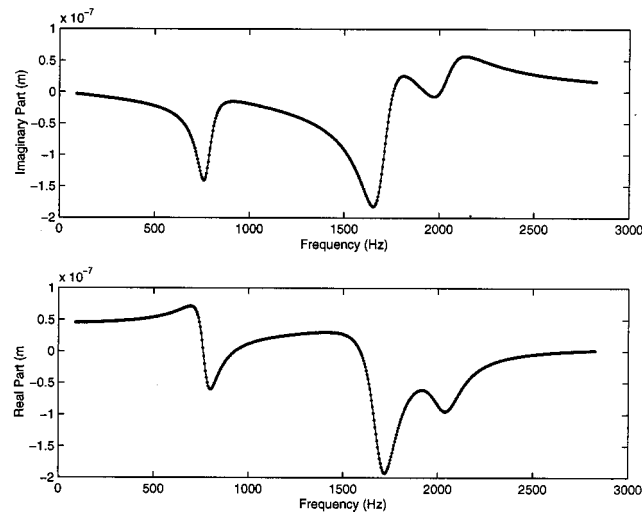


**Fig. 3** Frequency content of the sun translation transients for the three planet gear system impulse test. Force impulses are applied only to the sun and carrier translational degrees of freedom.

**Table 2** Natural frequencies of the three planet gear system

Natural Frequency (Hz)	Mode Type				
	Translation	Rotation	Translation	Rotation	Translation
Computational Model	780	1104	1695	1743	2145
Analytical Model	769	1119	1728	1771	2121
Difference (%)	1.4	-1.3	-1.9	-1.6	1.1

**Table 3** Natural frequencies of the four planet gear system

Natural Frequency (Hz)	Mode Type					
	Translation	Rotation	Planet	Translation	Rotation	Translation
Computational Model	778	1144	1729	1676	1723	2110
Analytical Model	769	1156	1690	1710	1781	2175
Difference (%)	1.2	-1.0	2.3	-2.0	-3.3	-3.0

identify the natural frequencies and vibration modes. Figure 3 shows typical frequency content of the sun transient response for the three planet gear system. The computational and analytical [4] natural frequencies agree well with a maximum difference of 3.3 percent (Tables 2 and 3). Representative vibration modes are shown in [4,8]. The lumped parameter masses, moments of inertia and mesh stiffness used in the analytical model are  $m_{\text{sun}} = 0.40$  kg,  $m_{\text{planet}} = 0.66$  kg,  $m_{\text{carrier}} = 5.43$  kg,  $J_{\text{sun}} = 0.483 \times 10^{-3}$  kg-m<sup>2</sup>,  $J_{\text{planet}} = 1.27 \times 10^{-3}$  kg-m<sup>2</sup>,  $J_{\text{carrier}} = 49.7 \times 10^{-3}$  kg-m<sup>2</sup>, and  $k_{\text{mesh}} = 350 \times 10^6$  N/m; all bearing stiffnesses are  $k_{\text{bearing}} = 87.6 \times 10^6$  N/m. Notice from Fig. 3 that force excitation of the sun gear excites only translational modes. Analogously, torque excitation of the sun gear excites only rotational modes. Tables 2 and 3 show that the translational and rotational natural frequencies are almost the same for the three and four planet systems. Planet modes occur only for systems with four or more planets [4].

Because the above natural frequencies are calculated directly from dynamic response (as opposed to an eigensolution), the excellent agreement with the analytical eigensolution builds confidence in the model's ability to capture the dynamic response of this multi-mesh system.

### 4 Dynamic Response Under Operating Conditions

**4.1 Speed Sweep.** To study the dynamic behavior of the planetary gear system under operating conditions, dynamic analyses are conducted over a range of sun speeds from 0–2500 rpm. The mesh frequency, which is related to sun speed by  $f_m = [Z_s Z_r / (Z_s + Z_r)] f_s$  where  $Z_{s,r}$  are numbers of teeth on the sun and ring, ranges from 0–880 Hz. A constant torque input of 1130 N-m (10000 lb-in) is applied at the sun gear. The nominal sun operating speed and torque for this helicopter system are 1600 rpm and 1413 N-m (12500 lb-in).

Figures 4–6 show the steady state frequency response amplitudes for the radial, tangential and rotational deflections of a planet in the four planet configuration (radial and tangential de-

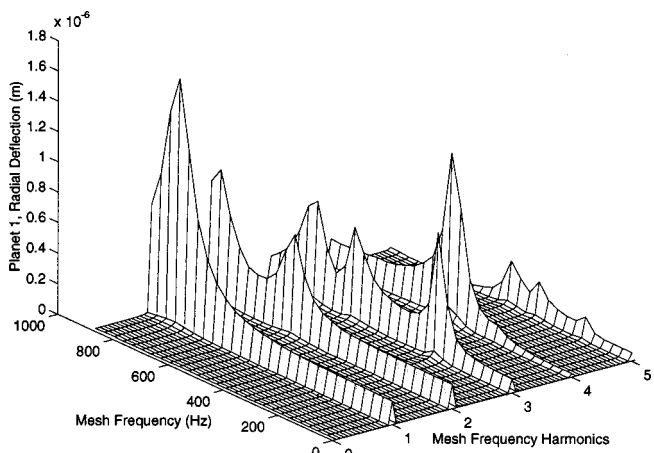


**Fig. 4** Frequency response amplitude of the planet radial deflection at various speeds for a sun torque of 1130 N-m (10000 lb-in) in a four planet gear system

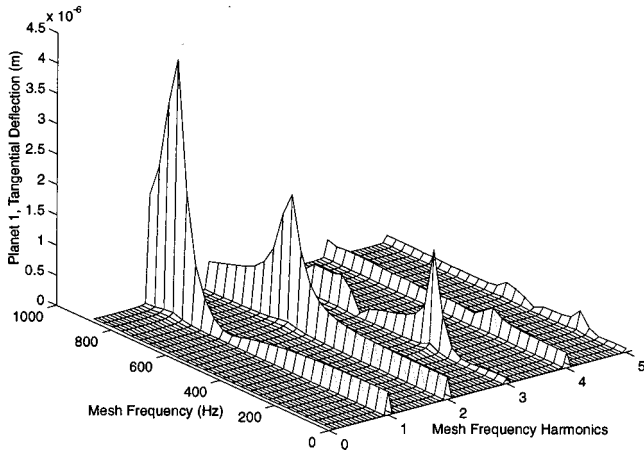


**Fig. 5** Frequency response amplitude of the planet tangential deflection at various speeds for a sun torque of 1130 N-m (10000 lb-in) in a four planet gear system

flections are with respect to a rotating, carrier-fixed basis). The deflections are those of the rigid bearing races of Fig. 2 and represent overall component motions. As the gears rotate, the dynamic tooth mesh forces are periodic at the mesh frequency. Accordingly, the calculated response has spectral content only in integer mesh frequency harmonics of the fundamental tooth mesh frequency for the range of operating speeds considered. This result is consistent with the static transmission error excitation model used in lumped-parameter representations. Manufacturing tolerances in practical systems introduce additional spectral content not captured in the perfect geometry of this model. The peaks correspond to resonant response at the natural frequency  $\omega_n$  excited in the  $l$ th mesh frequency harmonic, and they occur at mesh frequencies of  $(\omega_n/l)$ . This is evident from Fig. 7 where the planet radial deflection of Fig. 4 is re-plotted with a dimensional frequency axis; all resonant peaks clearly occur at the system natural frequencies. No data is plotted in the lower triangular region of Fig. 7 because only frequency content through the fifth harmonic is included.

The resonant peaks corresponding to different natural frequencies are not excited in all the mesh frequency harmonics. Consider Fig. 8, for example, where the planet rotational response of Fig. 6 is presented such that the individual harmonics are more clear. The first natural frequency at 788 Hz, which is associated with a

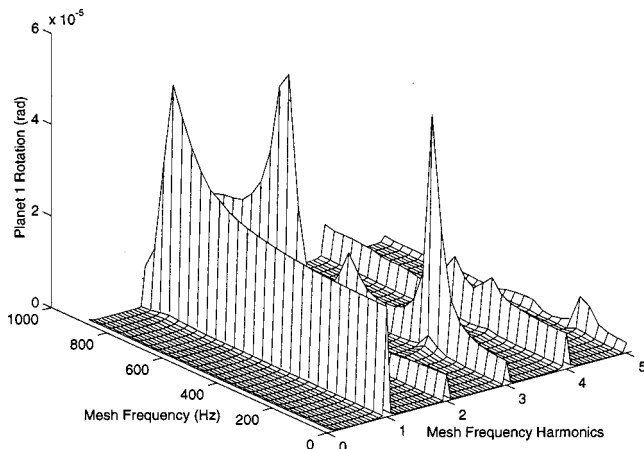


**Fig. 6** Frequency response amplitude of the planet rotational deflection at various speeds for a sun torque of 1130 N-m (10000 lb-in) in a four planet gear system

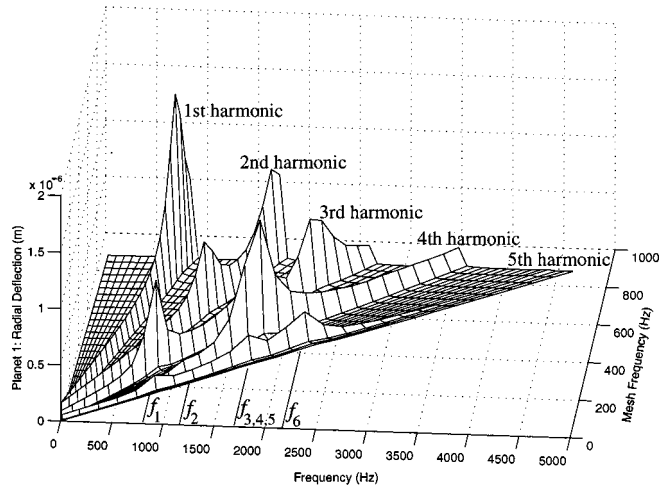


**Fig. 7** Frequency response amplitude of the planet radial deflection at various speeds for a sun torque of 1130 N-m (10000 lb-in) in a four planet gear system.  $f_i$  denotes the natural frequencies of the system.

translational mode, shows a resonant peak at a mesh frequency of 778 Hz. Resonant peaks corresponding to this translational mode also occur in the third and fifth harmonics at one-third and one-fifth of this speed, respectively. In contrast, no resonant peaks occur in the second, fourth or any even mesh frequency harmonic. The second natural frequency at 1144 Hz is associated with a rotational vibration mode. Resonant peaks corresponding to this rotational mode are present in the second and fourth harmonics at approximately one-half and one-fourth of the mesh frequency of 1144 Hz. Resonant peaks for this mode are present in all the even mesh frequency harmonics and absent from all the odd harmonics. The translational deflection of the sun gear, which occurs only when a translational mode is excited, contains only odd mesh frequency harmonics with no response in the even harmonics (Fig. 9). Similarly, rotational deflection of the sun gear has response only in the even harmonics with no response in the odd harmonics (Fig. 10).

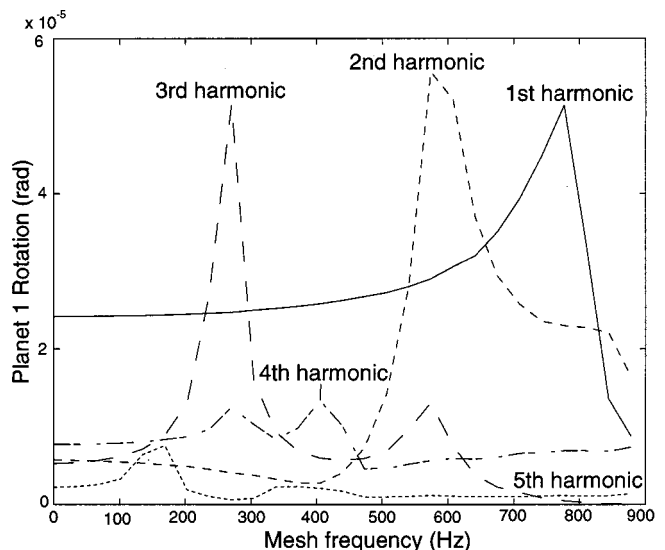


**Fig. 8** Frequency response amplitude of the planet rotational deflection of Fig. 6 presented such that the individual harmonics are clarified

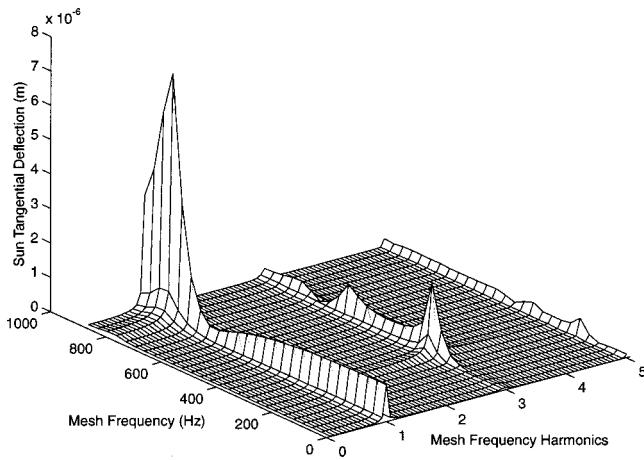


**Fig. 9** Frequency response amplitude of the sun tangential deflection at various speeds for a sun torque of 1130 N-m (10000 lb-in) in a four planet gear system

This peculiar behavior where particular modes are excited in some mesh frequency harmonics but not others is consistent with analytical predictions that address the practice of ‘planet phasing’ to suppress particular vibration modes in planetary gear response [18–20]. These results are summarized in Table 4 for equally spaced planets. The parameter  $k$  is defined as  $k = \text{mod}(lZ_s/N)$ , where  $l$  denotes the harmonic of mesh frequency,  $Z_s$  denotes the number of teeth on the sun gear, and  $N$  denotes the number of planets. The planets in the four planet system are not equally spaced but pairs of planets lie along diameters. In this case, the criteria for excitation of a particular mode in a specific harmonic are given by the following rules [20]: 1) For even values of  $lZ_s$ , translational modes are not excited and rotational modes are excited; 2) For odd values of  $lZ_s$ , translational modes are excited and rotational modes are not excited. For this four planet system with  $Z_s = 27$ , the translational modes are excited in only the odd mesh frequency harmonics whereas the rotational modes are excited in only the even mesh frequency harmonics. This is consistent with the presented results. These rules also explain why the sun gear translational response is present in only the odd mesh frequency harmonics and the sun gear rotational response is present in only the even mesh frequency harmonics. Notice that, consistent with the decoupled translational and rotational nature of

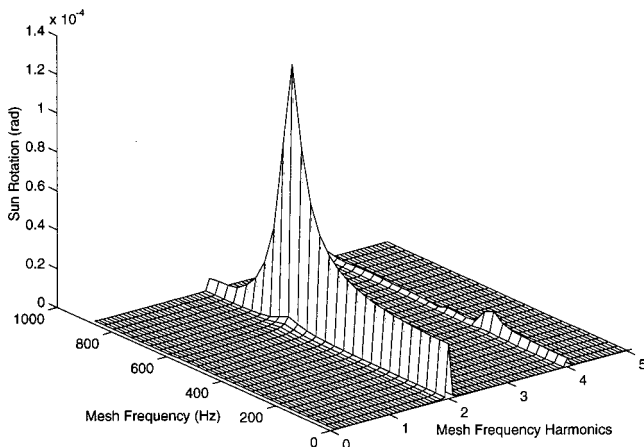


**Fig. 10** Frequency response amplitude of the sun rotational deflection at various speeds for a sun torque of 1130 N-m (10000 lb-in) in a four planet gear system

**Table 4** Conditions for different types of vibration modes to be excited for a planetary gear system with equally spaced planets. The quantity  $k = \text{mod}(lZ_s/N)$  depends on the number of planets  $N$ , the number of teeth on the sun gear  $Z_s$ , and the mesh frequency harmonic  $l$ .

$k$	Excitation of Vibration Modes
0	Translational modes not excited, Rotational modes excited.
$1, N - 1$	Translational modes excited, Rotational modes not excited.
$k \neq 0, 1, N - 1$	Rotational and translational modes not excited.

the vibration modes, all rotational mode resonant peaks are absent from the sun translational response, and all translational mode peaks are absent from the rotational response.

A speed sweep carried out for the system with three equally spaced planet gears shows different behavior. Figure 11 shows the

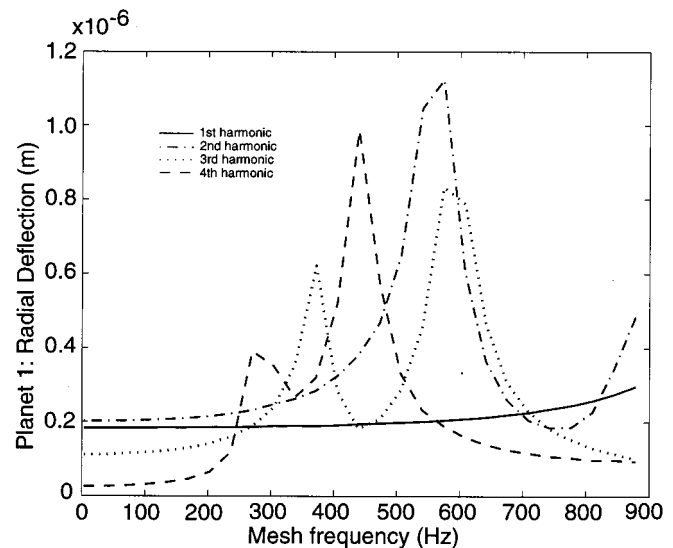
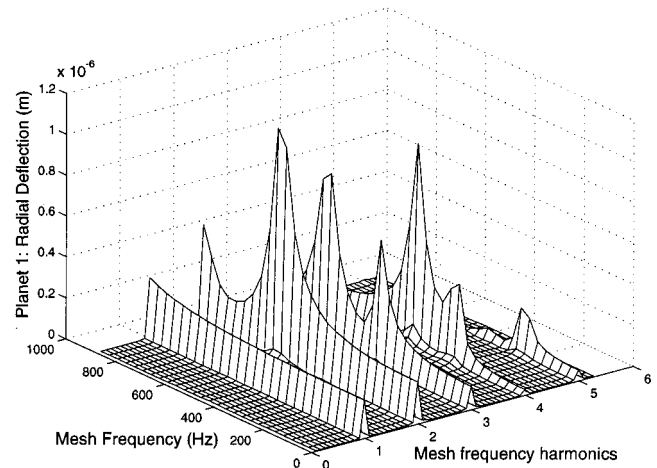


**Fig. 11** Frequency response amplitude of the planet radial deflection at various speeds for a sun torque of 1130 N-m (10000 lb-in) in a three planet gear system

translational deflection of a planet at different speeds. The resonant peaks corresponding to the translational mode natural frequencies at 780 Hz, 1695 Hz and 2145 Hz are absent in all the mesh frequency harmonics, whereas the resonant peaks corresponding to the rotational mode natural frequencies at 1104 Hz and 1743 Hz are observed in all the mesh frequency harmonics. The sun gear translation is zero at all times. This behavior is as expected from the planet phasing analysis summarized in Table 4 because  $k = \text{mod}(lZ_s/N) = 0$  for any  $l$  with  $Z_s = 27$  and  $N = 3$ .

As discussed previously, the dynamic forces at the tooth mesh are calculated internally and do not require external specification of mesh stiffness variation, static transmission error or the like. Nothing in the model predisposes the solution to exhibit the distinctive presence and absence of the various modes in different harmonics. That the computed dynamic response predicts these phenomena indicates that the approach accurately models the dynamic mesh forces and contact mechanics.

**4.2 Torque Sensitivity of Dynamic Response.** Avoidance of resonant response is not feasible when the planetary gear system operates across a wide speed range. Proper design of variable torque systems requires knowledge of the torque sensitivities of the resonant response. How the input torque changes the resonant amplitudes of the different types of modes is studied in this section.

The static transmission error of a single mesh gear pair is frequently used to represent the dynamic excitation under operating conditions in lumped-parameter models, though this modeling is considerably less developed for planetary gears. From this point of view, static response amplitudes are a possible measure of dynamic response in planetary gears, and one might expect that the static and dynamic responses show similar sensitivity to torque changes. To characterize the torque sensitivity of the *static* response, a torque sweep is carried out for a range from 113 N-m to 1356 N-m (1000 lb-in to 12000 lb-in) under static conditions. RMS values of the sun gear deflections about their mean are obtained over one tooth mesh cycle. Figure 12 compares the sun gear rotational and translational deflections with increasing input torque. In order to compare *changes* in the translational and rotational response with varying torque, the RMS values of these deflections at differing torques are normalized by their corresponding values at 113 N-m. The rotational deflection increases more rapidly than the translational deflection across the entire

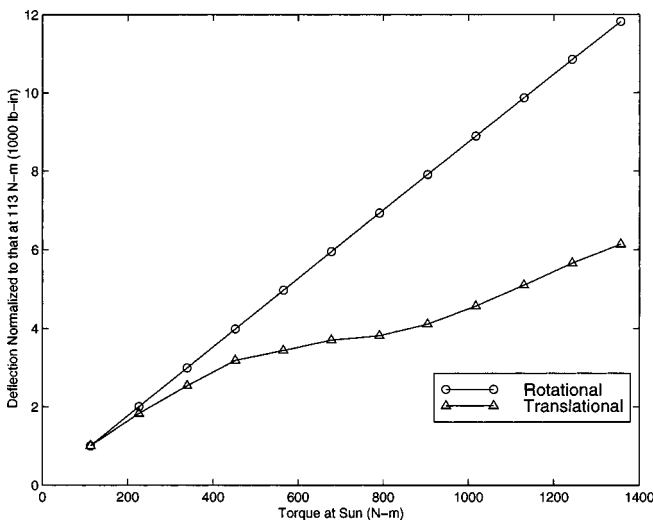


Fig. 12 Comparison of the change in the RMS sun gear rotational and translational deflections as the torque is increased. These are the results of static analyses.

torque range. This *static* analysis suggests that the *dynamic* rotational and translational mode responses may have substantially different sensitivities to the input torque.

To study the torque sensitivity of the resonant amplitudes, speed sweeps are performed for four input torques: 565 N-m, 1130 N-m, 1695 N-m, and 2260 N-m (i.e., 5000 lb-in, 10000 lb-in, 15000 lb-in and 20000 lb-in). The magnitudes of the resonant peaks corresponding to different vibration modes are compared. The first translational mode (778 Hz) and rotational mode (1144 Hz) natural frequencies (Table 3) are well separated, and the magnitudes of the corresponding resonant peaks are minimally affected by other vibration modes. The torque sensitivity of these vibration modes can thus be studied precisely.

Figures 13 and 14 show the magnitudes of the resonant peaks corresponding to the translational mode at 778 Hz and the rotational mode at 1144 Hz for a range of torques. Figure 13 shows results for the sun gear response; Fig. 14 shows similar results for the planet gear. The amplitudes of the resonant peaks at various torques are normalized to their corresponding values at 565 N-m (5000 lb-in). As discussed earlier, the translational modes show resonant response in odd harmonics only whereas the rotational modes show resonant response in even harmonics only. The peak resonant amplitudes of the rotational mode grow much faster with increasing torque than the translational mode amplitudes. Similar behavior, not shown in the figure, is observed for the translational mode natural frequency at 2110 Hz; its peak resonant response increases at a slower rate than the rotational mode at 1144 Hz. The other three natural frequencies (1676 Hz, 1723 Hz, and 1729 Hz) are closely spaced, and changes in these resonant amplitudes can not be isolated.

To confirm this behavior on a different system, we reduced the bearing stiffnesses and increased the planet moments of inertia. The lowest translational and rotational mode natural frequencies are well separated at 622 Hz and 782 Hz, respectively. Plots analogous to Figures 13 and 14 show remarkably similar behavior. The rotational mode resonant peaks increase faster with increased torque than those for translational modes.

The foregoing results indicate that rotational modes are more sensitive to changes in the input torque than translational modes. In this regard, the dynamic response follows the trend shown by the static response. Hence, the torque sensitivity of the static response, which can be studied with considerably less experimental and computational effort, provides an estimate for the sensitivity of the dynamic response. This behavior mimics that of single

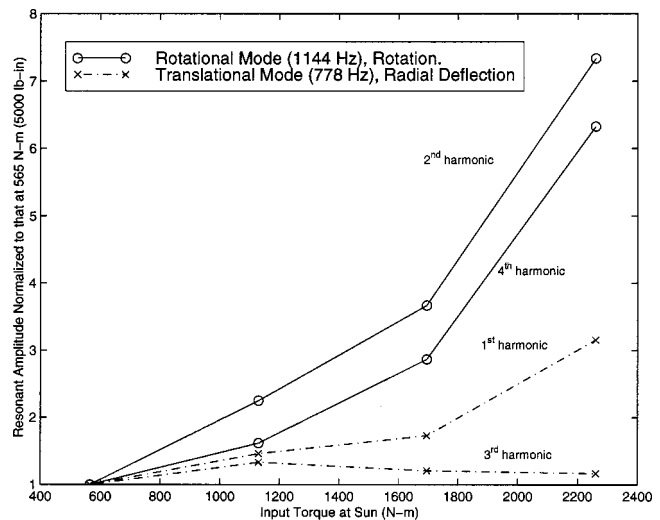
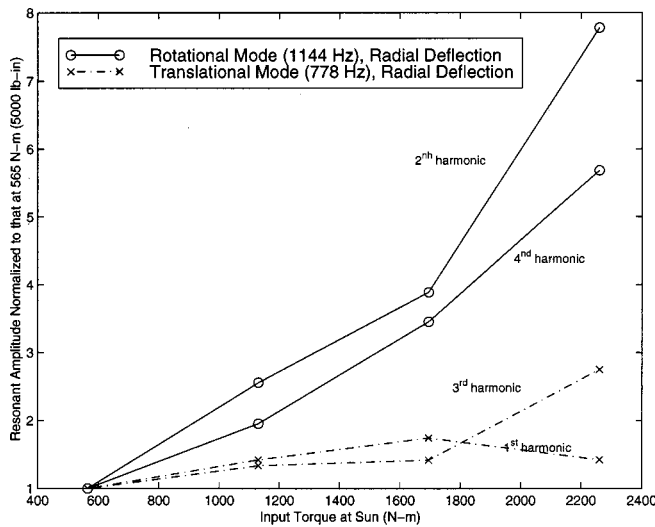


Fig. 13 Comparison of the peak sun gear resonant response for the 1) rotational mode at 1144 Hz, and 2) translational mode at 778 Hz. Solid curves denote sun rotation and dashed curves denote sun translation.



**Fig. 14 Comparison of the peak planet gear resonant response for the 1) rotational mode at 1144 Hz, and 2) translational mode at 778 Hz. The curves denote planet radial deflection for both modes.**

mesh gear pairs. To better quantify the relationship between static and dynamic response, one needs to examine the spectral content of the static responses of Fig. 12. Additionally, the torque sensitivity findings may depend on tooth modifications.

## 5 Summary and Conclusions

This study presents comprehensive dynamic response results for a planetary gear system under a range of operating speeds and torques. The finite element/contact mechanics analysis employed offers significant advantages in modeling the nonlinear tooth contact and mesh stiffness variation that drive the vibratory motions. The unique contact modeling permits dynamic *response* analyses (as opposed to the much simpler static and natural frequency/vibration mode analyses) with a reasonable number of degrees of freedom. In particular, the multiple meshes of planetary gears are handled naturally, and no a priori specification of the dynamic mesh forces is required. The presented results expose dynamic phenomena and provide comprehensive data for benchmarking simpler lumped parameter models. Three indicators, none of which are pre-imposed in the modeling, build confidence in the results: 1) excellent agreement of the natural frequencies and vibration modes as determined from transient dynamic response with results from an analytical model, 2) the expected excitation of resonance at speeds where the mesh frequency or its harmonics coincide with a natural frequency, and 3) consistency of the predicted presence and absence of certain modes in the response according to 'planet phasing' predictions.

For the range of operating speeds and torques considered and in the absence of geometric imperfections, the response has spectral content only at mesh frequency ( $\omega_m$ ) and its harmonics. Resonance conditions *may* be excited by the  $l$ th mesh frequency harmonic when a natural frequency coincides with  $l\omega_m$ . Whether or not a particular harmonic excites resonance in a specific mode is

predicted by simple analytical expressions depending on the type of mode (rotational or translational), the mesh frequency harmonic  $l$ , the number of planets, and the number of sun gear teeth.

Response in rotational and translational modes have different sensitivity to changes in operating torque. The resonant amplitude of rotational modes changes more rapidly with torque than that for translational modes. These dynamic results are consistent with static analysis, which may provide a simpler analytical and experimental means to assess torque sensitivity of the vibration. For the unmodified gear teeth in this model, the response increases monotonically with torque.

## Acknowledgments

The authors thank T. L. Krantz of the Army Research Lab for helpful discussions and advice throughout the work. This material is based on work supported by the NASA Glenn Research Center under grant NAG3-11979 and the U.S. Army Research Office under grant DAAD19-99-1-0218.

## References

- [1] Cunliffe, F., Smith, J. D., and Welbourn, D. B., 1974, "Dynamic Tooth Loads in Epicyclic Gears," *ASME J. Eng. Ind.*, **95**, pp. 578–584.
- [2] Botman, M., 1976, "Epicyclic Gear Vibrations," *ASME J. Eng. Ind.*, **97**, pp. 811–815.
- [3] Kahraman, A., 1994, "Natural Modes of Planetary Gear Trains," *J. Sound Vib.*, **173**, pp. 125–130.
- [4] Lin, J., and Parker, R. G., 1999, "Analytical Characterization of the Unique Properties of Planetary Gear Free Vibration," *J. Vib. Acoust.*, **121**, pp. 316–321.
- [5] Lin, J., and Parker, R. G., 2000, "Structured Vibration Properties of Planetary Gears with Unequally Spaced Planets," *J. Sound Vib.*, **233**, pp. 921–928.
- [6] Lin, J., and Parker, R. G., 1999, "Sensitivity of Planetary Gear Natural Frequencies and Vibration Modes to Model Parameters," *J. Sound Vib.*, **228**, pp. 109–128.
- [7] Kahraman, A., 1994, "Load Sharing Characteristics of Planetary Transmissions," *Mech. Mach. Theory*, **29**, pp. 1151–1165.
- [8] Kahraman, A., 1994, "Planetary Gear Train Dynamics," *ASME J. Mech. Des.*, **116**, pp. 713–720.
- [9] Velez, P., and Flamand, L., 1996, "Dynamic Response of Planetary Trains to Mesh Parametric Excitations," *ASME J. Mech. Des.*, **118**, pp. 7–14.
- [10] Saada, A., and Velez, P., 1995, "An Extended Model for the Analysis of the Dynamic Behavior of Planetary Trains," *ASME J. Mech. Des.*, **117**, pp. 241–247.
- [11] Valco, M. J., 1992, "Planetary Gear Train Ring Gear and Support Structure," Doctoral Dissertation, Cleveland State University.
- [12] Gradu, M., Langenbeck, K., and Breunig, B., 1996, "Planetary Gears with Improved Vibrational Behavior in Automatic Transmissions," *VDI BER-ICHTE NR 1996*, pp. 861–879.
- [13] Vijayakar, S., 1991, "A Combined Surface Integral and Finite Element Solution for a Three-Dimensional Contact Problem," *Int. J. Numer. Methods Eng.*, **31**, pp. 525–545.
- [14] Vijayakar, S. M., Busby, H. R., and Houser, D. R., 1988, "Linearization of Multibody Frictional Contact Problems," *Comput. Struct.*, **29**, pp. 569–576.
- [15] Parker, R. G., Vijayakar, S. M., and Imajo, T., 2000, "Nonlinear Dynamic Response of a Spur Gear Pair: Modeling and Experimental Comparisons," *J. Sound Vib.*, in press.
- [16] Blankenship, G. W., and Kahraman, A., 1996, "Gear Dynamics Experiments, Part-I: Characterization of Forced Response," *Proc. of ASME Power Transmission and Gearing Conference*, San Diego.
- [17] Krantz, T. L., 1992, "Gear Tooth Stress Measurements of Two Helicopter Planetary Stages," *NASA Technical Memorandum 105651*, AVSCOM Technical Report 91-C-038, pp. 1–8.
- [18] Seager, D. L., 1975, "Conditions for the Neutralization of Excitation by the Teeth in Epicyclic Gearing," *J. Mech. Eng. Sci.*, **17**, pp. 293–298.
- [19] Kahraman, A., and Blankenship, G. W., 1994, "Planet Mesh Phasing in Epicyclic Gear Sets," *Proc. of International Gearing Conference*, Newcastle, UK, pp. 99–104.
- [20] Parker, R. G., 2000, "A Physical Explanation for the Effectiveness of Planet Phasing to Suppress Planetary Gear Vibration," *J. Sound Vib.*, **236**, pp. 561–573.